

Dalton Transactions

Accepted Manuscript



This is an *Accepted Manuscript*, which has been through the Royal Society of Chemistry peer review process and has been accepted for publication.

Accepted Manuscripts are published online shortly after acceptance, before technical editing, formatting and proof reading. Using this free service, authors can make their results available to the community, in citable form, before we publish the edited article. We will replace this *Accepted Manuscript* with the edited and formatted *Advance Article* as soon as it is available.

You can find more information about *Accepted Manuscripts* in the [Information for Authors](#).

Please note that technical editing may introduce minor changes to the text and/or graphics, which may alter content. The journal's standard [Terms & Conditions](#) and the [Ethical guidelines](#) still apply. In no event shall the Royal Society of Chemistry be held responsible for any errors or omissions in this *Accepted Manuscript* or any consequences arising from the use of any information it contains.

FULL PAPER

Novel layered crystalline organic polymer-inorganic hybrid material comprising calcium phosphate with unique architectures for superior performance catalyst support†

Cite this: DOI: 10.1039/x0xx00000x

Received 00th January 2012,
Accepted 00th January 2012

DOI: 10.1039/x0xx00000x

www.rsc.org/

Jing Huang,^{a,b} Mei Tang,^a Xin Li,^a Guo Zhen Zhong^a and Chang Ming Li^{a*}

A organic copolymer-inorganic hybrid material, calcium phosphonate-phosphate (CaPS-PVPA) was fabricated under mild conditions. In particular, CaPS-PVPA was not prepared with traditional methods such as a hydrothermal one, but with amorphous reactions for a simple, fast, cost-effective and environmentally benign approach. Characterization shows that CaPS-PVPA is layered crystalline mesoporous material, and could be readily used as a catalytic support. A catalyst with immobilization of chiral salen Mn (III) onto CaPS-PVPA demonstrates superior catalytic disposition (conv, >99% and ee, >99%), which offers great potential for industry scale applications.

Introduction

Metal organic frameworks are enjoying widespread contemporary interest by virtue of their applications in areas of catalysis, optical materials, membranes, and sorption.¹⁻¹¹ The diverse properties of these materials reflects a vast compositional range, thus providing great potential to design novel functional materials, of which the properties from both inorganic and organic realms can combine in a complimentary way,¹²⁻¹³ thus leading to unusual structures with unique properties while opening an avenue to design multifunctional materials.

Our previous works have reported a series of organic-inorganic hybrid zirconium phosphonate-phosphates as catalysts or catalyst supports, such as solid base catalyst $Zr(O_3PCH_2NCH_2NR^1R^2)_2 \cdot H_2O$, layered amorphous and crystalline zirconium [N-(phosphonomethyl)morpholine-phosphate] and $Zr(HPO_4)[O_3PCH_2N(CH_2CH_2)_2O] \cdot nH_2O$.¹⁴⁻¹⁵ In addition, zirconium phosphate-phosphonate derivatives have been synthesized as supports for the immobilization of chiral salen Mn(III), for instance

zirconium oligostyrenylphosphonatephosphate (ZSPP), zirconium poly (styrene-isopropenylphosphonate)-phosphate (ZPS-IPPA), zirconium poly (styrene-phenylvinylphosphonate)-phosphate (ZPS-PVPA) as well as zinc poly (styrene-phenylvinylphosphonate)-phosphate (ZnPS-PVPA).¹⁶⁻²⁰

Currently in the orthopedic and dental industry, calcium phosphate (CaP) materials are the most widely used and studied resorbable bone simulate due to their compositional similarity to natural bone and excellent biocompatibility. Presently, clinical utilization of CaPs can be found in a broad range of products including coatings on metallic implants, bone cements and grafting materials.²¹

In this work, CaPS-PVPA 1-7 are synthesized from co-polymer styrene-phenylvinylphosphonic acid, calcium nitrate tetrahydrate and sodium dihydrogen phosphates treated with mixtures of phosphonate and phosphate at different ratios. The method is simple, economic, environmentally friendly and completely different from the traditional approaches, which usually undergo a direct reaction of phosphonic acid with a metal source by a hydrothermal process, or by heating to reflux appropriate solutions, or by making metal salts contact with molten phosphonic acid. The catalytic performance of CaPS-PVPA-supported chiral salen Mn (III) is investigated primarily in asymmetric epoxidation of non-functionalized olefins to compare with those supported on ZSPP or ZPS-PVPA. Thorough analysis of the results proposes the hypothesized structure of CaPS-PVPA and a confinement effect of nanopores

^a Institute for Clean Energy & Advanced Materials, Southwest University, Chongqing 400715, PR China. E-mail: hj41012@163.com; Tel: +86 23 68254672; Fax: +86 23 68254672.

^b Research Center for Advanced Computation, Xihua University; School of Physics and Chemistry, Xihua University, Chengdu, 610039, PR China.

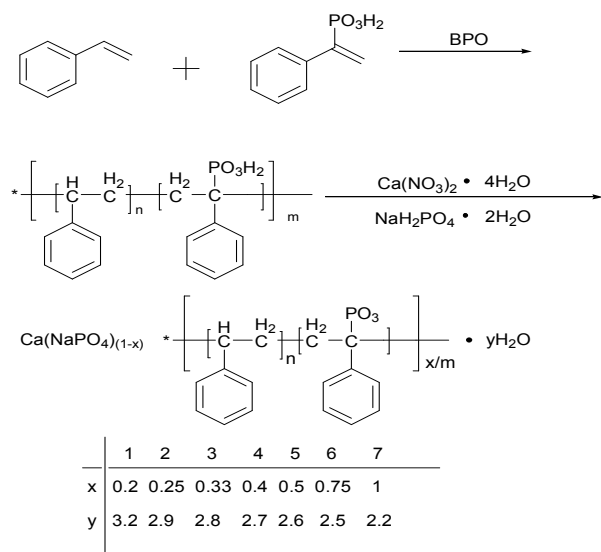
†Electronic Supplementary Information (ESI) available: FT-IR, XRD, the hypothesized structure of the copolymer, Solid UV-vis spectrum. See DOI: 10.1039/b000000x/

to offer physic-chemical insights for exploration of novel properties of CaPS-PVPA as functional materials in potential important applications as catalyst support.

Experiment

Materials and instruments

All chemicals and reagents in this work were analytical grade and used as received. All the solvents were further purified before use. Chiral salen ligand and chiral homogeneous catalyst salen Mn(III) were synthesized according to the literature procedures,²² and further confirmed by analysis of IR spectra.²³ CaPS-PVPA was synthesized as described in Scheme 1.



Scheme 1. synthesis of CaPS-PVPA 1-7.

Synthesis of styrene-phenylvinylphosphonic acid copolymer (PS-PVPA)

1-Phenylvinyl phosphonic acid (PVPA) was synthesized according to literature²⁴ and its structures were confirmed by ¹H NMR, ³¹P NMR and FT-IR. ¹H NMR (CDCl₃): 6.06 (d, 1H), 6.23 (d, 1H), 7.26-7.33 (m, 3H), 7.48 (m, 2H). ³¹P NMR (CD₃OD): 15.9. IR (KBr): 2710, 2240, 1500, 1200, 1040, 950, 780, 720, 700 cm⁻¹.

1-Phenylvinyl phosphonic acid (4 g, 21.7 mmol), styrene (20 mL, 173.9 mmol), ethyl acetate (150 mL) and dibenzoyl peroxide (BPO, 1.0g, 4.7 mmol) were used for preparation of PS-PVPA copolymer as literature.¹⁸ GPC: Mn = 39729.43, m = 38.3, n = 8.2, Mw/Mn = 2.

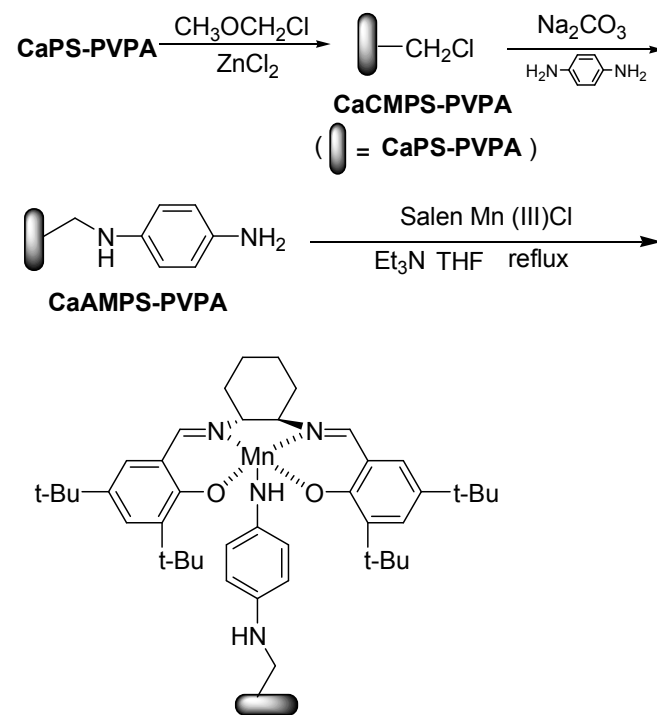
Synthesis of Calcium Poly(styrene-phenylvinylphosphonate)-phosphate (CaPS-PVPA)

Sodium dihydrogen phosphate (0.62g, 4mmol) in 3 mL of deionized water was added to PS-PVPA solution (1.0g, 1mmol) for preswelling in THF at room temperature for 30 min with stirring. Thereafter, calcium nitrate tetrahydrate (1.2g, 5mmol) in 3 mL of deionized water was added in while gradually rising temperature to 66 °C and then retaining for 4 h, followed by

cooling down and then evaporating under reduced pressure. Then ivory yellow solid calcium poly(styrene-phenylvinylphosphonate)-phosphate 1 was filtered, washed with deionized water and dried at 80 °C for 12h in vacuum. Ivory yellow CaPS-PVPA 2-7 were prepared according to the similar procedure.

Synthesis of the heterogeneous catalyst

CaPS-PVPA-supported chiral Mn (III) was synthesized according to the similar literature procedure.²⁵(Scheme 2)



Scheme 2. Synthesis of the supported catalyst.

Chemical analysis

In a white porcelain crucible, a sample of 60 mg CaPS-PVPA 3 was put in and was heated up to 700 °C for 5h in a Muffle furnace for decomposition. Subsequently, 20 mL of hydrochloric acid (1:1) was added into the porcelain crucible and heated to boiling for 30 min on the electric furnace. The sodium content in the resulted solution was determined by AAS.

Asymmetric epoxidation

The activity of the prepared catalysts were tested for the epoxidation of non-functionalized olefins in CH₂Cl₂ at -20 °C for 6 h using *m*-CPBA/NMO. After reaction, Na₂CO₃ (4 mL, 1.0M) was added to quench the reaction.

Results and discussion

Na content of CaPS-PVPA 3

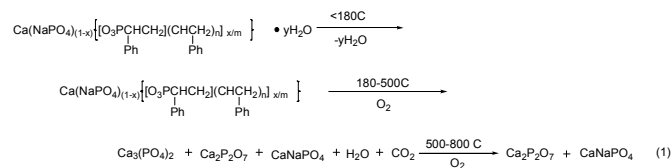
The sodium content in CaPS-PVPA 3 is 4.6%, which is 0.3% lower than that of theoretical values. This can be ascribed to the surface-bound or intercalated water inducing the augmentation of the molecular weight.

Infrared spectroscopy

FT-IR spectroscopy is used to characterize and compare CaPS-PVPA 1-7 as shown in Fig. S1. The strong and wide absorption band extending from 3090 cm^{-1} to 3750 cm^{-1} and centering at 3500 cm^{-1} by virtue of $-\text{OH}$ verifies the presence of surface-bound or intercalated water. The transmissions around 2900 cm^{-1} of the samples are due to C-H bond stretching vibrations of alkyl groups. In the range of $1600\text{--}1450\text{ cm}^{-1}$ and $760\text{--}690\text{ cm}^{-1}$, the absorption bands are attributed to the characteristic absorptions and the flexing vibration of phenyl group, respectively. The other common prominent bands at 1145 , 1089 , and 986 cm^{-1} can be assigned to R-PO_3^{2-} phosphonate stretching vibrations. The adsorptions at 1201 , 1144 , and 1077 cm^{-1} are ascribed to the phosphonate and phosphate stretching vibrations. These FT-IR spectra indicate that CaPS-PVPA are prepared successfully.

Thermal gravimetric analysis

The thermogravimetric weight loss curves for CaPS-PVPA 1, 3, 5 in Fig. S2 indicate that these compounds lost surface-bound or intercalated water below $180\text{ }^\circ\text{C}$, and the process is endothermic as usual. The number of water molecules comprised in CaPS-PVPA is proportional to the ratio of inorganic phosphate. After dehydration, the apparent weightlessness in the temperature range of $180\text{--}500\text{ }^\circ\text{C}$ is owing to the desintegration of the appended organic fragments. Accompanying with the volatilization of organic segments, calcium phosphonates are transformed to calcium phosphate. Ultimately, there are small weight losses between 500 and $800\text{ }^\circ\text{C}$ by virtue of phase changes from layer to cubic $\text{Ca}_2\text{P}_2\text{O}_7$ and $\text{Ca}_3(\text{PO}_4)_2$. The corresponding reactions related to the whole



weight loss can be ones as shown in eq 1. On account of the losses of pendant organic moieties, it varied from 60.6% to 96.3%, which are either higher or lower than those of the theoretical values. It can probably be due to the different ratios of phosphonate to phosphate in the sample. The gel composition, reactive conditions as well as product composition are listed in Table 1. It can be deduced that the melting point of the samples increases with the percentage of phosphate in the sample. Moreover, the samples have enough thermal stability to be applied as catalyst supports, due to organic reactions of heterogeneous catalyst usually proceeded under $180\text{ }^\circ\text{C}$.

Table 1 Synthesis Conditions and Analysis for Compound 1-7

sample	synthetic conditions			Analysis		formula	
				EDAX	TGA		
	Ca(NO ₃) ₂ : NaH ₂ PO ₄ : PS-PVPA : H ₂ O	T (°C)	Time (h)	Zn : P	Organic moieties (%)		
1	5 : 4 : 1	450	66	4	1 : 1	60.6	Ca(NaPO ₄) _{0.78} [PS-PVPA] _{0.22} ·3.2H ₂ O
2	4 : 3 : 1	350	66	4	1 : 1	66.8	Ca(NaPO ₄) _{0.76} [PS-PVPA] _{0.24} ·2.9H ₂ O
3	3 : 2 : 1	250	66	4	1 : 1	74.4	Ca(NaPO ₄) _{0.66} [PS-PVPA] _{0.34} ·2.8H ₂ O
4	2.5 : 1.5 : 1 : 200	66	4	4	1 : 1	78.9	Ca(NaPO ₄) _{0.61} [PS-PVPA] _{0.39} ·2.7H ₂ O
5	2 : 1 : 1	150	66	4	1 : 1	83.9	Ca(NaPO ₄) _{0.48} [PS-PVPA] _{0.52} ·2.6H ₂ O
6	4 : 1 : 3	350	66	4	1 : 1	91.2	Ca(NaPO ₄) _{0.26} [PS-PVPA] _{0.74} ·2.5H ₂ O
7	1 : 1 : 1	550	66	4	1 : 1	96.3	Ca[PS-PVPA]·2.3H ₂ O

Powder XRD.

XRD patterns of CaPS-PVPA 3 in Fig. S3 indicate a lenient 001 peak, accompanying with other peaks at higher-order 00n peaks at larger angles and lower intensities such as at 26.42° and 30.20° . The sections of inorganic phosphate in CaPS-PVPA 1-6 exhibit similarity of XRD patterns as that of $\text{Ca}_3(\text{PO}_4)_2$ at the vicinity of 26.42° and 30.20° . Then, XRD patterns of CaPS-PVPA 1-6 close to 19.76° are proximate to that of CaPS-PVPA 7, which is ascribed to the presence of calcium poly(styrene-phenylvinylphosphonate) in CaPS-PVPA 1-6. Consequently, it can be concluded that CaPS-PVPA 1-6 are rather calcium poly(styrene-phenylvinylphosphonate)-phosphate hybrid materials than a blend of calcium inorganic phosphate and calcium poly(styrene-phenylvinylphosphonate).

Nitrogen adsorption-desorption isotherms

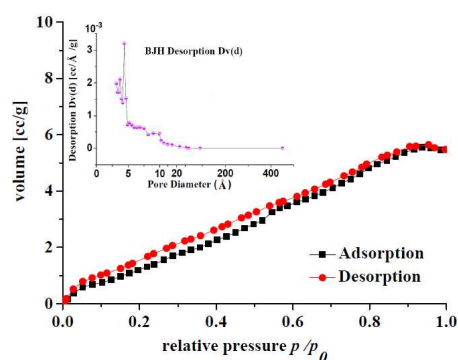


Fig. 1 Pore distribution of and the nitrogen adsorption-desorption isotherm CaPS-PVPA 3.

On account of the BET treatment of the isotherms, CaPS-PVPA 3 indicates low specific surfaces areas ($7.08\text{ m}^2/\text{g}$) and pore volume ($0.92 \times 10^{-2}\text{ cm}^3/\text{g}$) as well as average pore diameter (4.89 nm). The nitrogen adsorption-desorption isotherms of CaPS-PVPA 3 (Fig. 1) are type I, with a sharp increase in N_2 adsorption at higher P/P_0 values (~ 0.9) and a distinct hysteresis loop (type H2), with an almost parallel adsorption and desorption. With regard to the desorption isotherm of CaPS-PVPA 3 (Fig. 1), BJH analysis manifests a very broad pore size

distribution of pore size. The pore diameters of the particles are mainly distributed below 2 nm, and some particles are over 2 nm. The physical properties of 1, 3, 5 and 7 are listed in Table 2.

Table 2 Physical properties of 1, 3, 5 and 7

sample	Surface area ($\text{m}^2 \text{g}^{-1}$)	Pore volume ($\times 10^{-2} \text{cm}^3 \text{g}^{-1}$)	Average pore diameter (nm)
1	3.56	0.46	5.16
3	7.08	0.92	4.89
5	6.49	0.85	4.83
7	5.88	0.70	4.75

Meanwhile, the size of the solvated Mn(salen)Cl complex is estimated to be 2.05-1.61 nm by MM2.²⁶ Thus, CaPS-PVPA 3 could offer enough room to accommodate the solvated chiral Mn(III)salen complexes. Moreover, the local environment inside the mesopores and pore size of CaPS-PVPA 3 have significant effects on the enantioselectivity of the epoxidation reaction, which is a crucial property as a catalyst support to immobilize salen Mn (III). The solid support with varied pore sizes is not only prone to secure the optimal pore size for efficient diffusion of reactant and product molecules, but also benefit to immobilization of the active metal complex such as chiral salen Mn (III).

Surface morphology

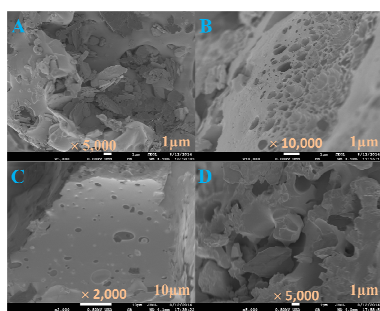


Fig. 2 FESEM image of layered CaPS-PVPA 1 (A), 3 (B), 5 (C) and 7 (D).

SEM images of CaPS-PVPA (Fig. 2) indicate that the diameters of the particles are in the range of microns and that the samples are composed of irregularly sized layered particles which are aggregates of many minor crystalline grains. The anomalous suborbicular segments are congregation of the parts of calcium inorganic phosphate in CaPS-PVPA; while inordinate plate layers are congregation of proportions of calcium poly(styrene-phenylvinylphosphonate) in CaPS-PVPA. And generous caves, holes, pores and channels also exist in every particle. In particularly, some micropores and secondary channels can increase the surface area of the catalyst and make substrates access to the catalytic active sites easily.²⁵

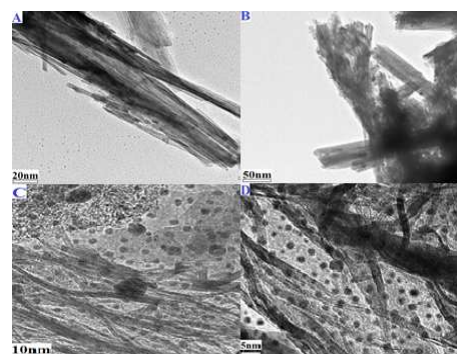


Fig. 3 TEM micrographs of CaPS-PVPA 3 (A-D).

TEM micrographs of CaPS-PVPA 3 (Fig. 3) reveal that the areatus sections in a wide variety of sizes are ascribed to accumulation of parts of calcium inorganic phosphate in CaPS-PVPA and the zonary segments with different width are attributed to congregation of proportion of calcium poly(styrene-phenylvinylphosphonate) in CaPS-PVPA. And various shapes of channels, holes and canvums can also be discerned clearly. This demonstrates that more chances will be provided for substrates to approach the internal catalytic active sites in solution.

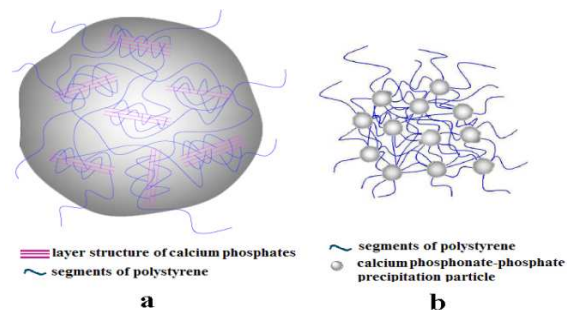


Fig. 4 hypothesized surface morphology of CaPS-PVPA

On account of the surface morphology, there are probably two kinds of gathering model. According to Fig.4a, it indicates that the two or more neighboring $-\text{PO}_3\text{H}_2$ groups (there is a polystyrene chain between and connected to them) are in same colloidal precipitation; while for Fig. 4b, it manifests that the two neighboring $-\text{PO}_3\text{H}_2$ groups (there is a polystyrene segment between and linked to them) are in different colloidal precipitations. In the aggregation procedure of the colloidal precipitation into larger particles, many precipitation particles link each other to form even larger hybrid CaPS-PVPA precipitation particles and a great deal of channels, holes and cavums with different volumes and shapes are gradually formed at the same time. Therefore, according to model **b**, different lengths and shapes of channels, holes and cavums will take shape; while for model **a**, smaller channels, holes and cavums may come into being and cover on the surface of the small precipitation particles.

Solid UV-vis spectrum

The absorbance UV-vis spectrum for CaPS-PVPA 3 displays a strong absorption around 277 nm (Fig. S4) which is attributed to the p-p* transition of the phenyl groups. There is another strong absorption around 335 nm which is assigned to the involvement of the charge transfer transitions from the O atoms of the phosphate or phosphonate to the empty 4s orbitals of the Ca²⁺ ions. On the other hand, the corresponding diffuse reflectance UV-vis spectrum also agrees with the results. In view of this, CaPS-PVPA 3 may be utilized in the field of shielding UV, such as sunscreen creams.

Steric effect of CaPS-PVPA

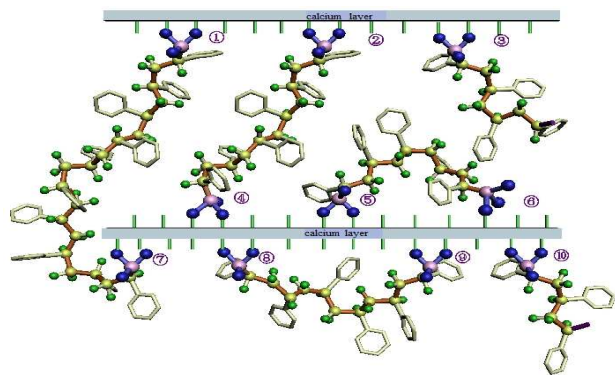


Fig. 5 The hypothesized layered structure of CaPS-PVPA 3 (green: H; blue: O; greenyellow: C; purple: P)

The hypothesized structure deduced for CaPS-PVPA 3 is displayed in Fig. 5 and its exact structure will be ascertained in the future. In the hypothesized models, some oxygen atoms of the hydroxyl groups or hydroxyl sodium in the inorganic phosphate sections are coordinated with calcium atom, making the calcium atoms self-assembled in the same plane, while the other oxygen atoms of the inorganic phosphate parts in CaPS-PVPA stretch over the surface of the calcium layer. Simultaneously, several types of conjugating modes of organic polymer phosphonate-PO₃H₂ (opp-PO₃H₂) are present in CaPS-PVPA: (1) Opp-PO₃H₂ ① is located on the interlayer surface of one calcium layer, coupled with another particle of CaPS-PVPA by a polystyrene segment. In other words, opp-PO₃H₂ ③ and its neighboring opp-PO₃H₂ are located in a different particle of CaPS-PVPA, which is as same as opp-PO₃H₂ ⑩ group. (2) Opp-PO₃H₂ group ② is connected to opp-PO₃H₂ ④ by a polystyrene section and is individually situated on the interlayer surface of the two adjacent calcium layers. In addition, the opp-PO₃H₂ group ① is perched on the interlayer surface of one calcium layer and linked to opp-PO₃H₂ group ⑦ by a polystyrene segment which lied on the surface of another contiguous calcium interlayer space. (3) Opp-PO₃H₂ group ⑤ and opp-PO₃H₂ group ⑥, which are conjunct to one another, located on the interlayer surface of the same calcium layer. The similar phenomenon occurs to opp-PO₃H₂ group ⑧ and opp-PO₃H₂ group ⑨. In general, there are at least three structure models of opp-PO₃H₂ shaped in CaPS-PVPA: (i) two contiguous opp-PO₃H₂ groups (there is a polystyrene segment between and joined to them) in the same particle are perched on

a diverse crystalline grain; (ii) two neighboring opp-PO₃H₂ groups are located on the different layer in the same crystalline grain; (iii) two adjacent opp-PO₃H₂ groups are situated on the same layer in the same crystalline grain. Accordingly, pores or channels with various sizes and shapes formed by appropriate modification of the styrene-phenylvinylphosphonic acid copolymer chain can contribute to the significant impact on the excellent catalytic activity discussed later.

Table 3 The interlayer distances or *d*-spacings of CaPS-PVPA 1–7 and Ca₃(PO₄)₂

sample	1	2	3	4	5	6	7	Ca ₃ (PO ₄) ₂
interlayer distances or <i>d</i> -spacings (Å)	35±1.5	35±1.2	35±1.8	35±1.6	35±1.7	35±1.9	35±1.1	3.18

On the other hand, the interlayer distances of CaPS-PVPA 1–7 (Table 3), which are just only one of the representative interlayer distance values, are not the same values as that of Ca₃(PO₄)₂ (3.18Å), but a set of all values are around 35 to 36 Å. These results also indicate that introducing of the chains of styrene-phenylvinylphosphonic acid copolymer causes certain deviations among CaPS-PVPAs. Meanwhile, different structures of opp-PO₃H₂ have different impacts on the interlayer distances of CaPS-PVPA. Shown in Fig. 5, the interlayer distances of CaPS-PVPA may be larger for the structure types of opp-PO₃H₂ (i) (two contiguous opp-PO₃H₂ groups in the same particle are perched on a diverse crystalline grain), and medium for the structure types of opp-PO₃H₂ (ii) (two neighboring opp-PO₃H₂ groups are located on the different layer in the same crystalline grain), as well as relatively narrower for the structure types of opp-PO₃H₂ (iii) (two adjacent opp-PO₃H₂ groups are situated on the same layer in the same crystalline grain). In addition, the interlayer distances of CaPS-PVPA 1–7 are nearly 32 Å broader than that of Ca₃(PO₄)₂ (3.18Å), probably due to the styrene-phenylvinylphosphonic acid copolymer chain making the calcium layer stretched.

Confinement effect of nanopores

As is known, the confinement effect of nanopores can contribute to a superior catalytic behavior from catalyst confined in nanopores.²⁷⁻³⁰ However, the confinement effect have not been well understood. This work could provide some fundamental insights. CaPS-PVPA can be produced by coprecipitation of the calcium in the presence of styrene-phenylvinylphosphonic acid (P-G) and phosphoric acid (P-OH), accompanying with the formation of a porous structure. Residue or side chain for opp-groups of P-G and inorganic phosphate P-OH in CaPS-PVPA are completely different in sizes, of which the opp-groups of P-G are fairly bulky and the inorganic phosphate P-OHs are relatively small. Then random distribution of the organic groups is usually involved in CaPS-PVPA to possess identical stoichiometry for all layers. In such a system, the interlayer spacing (*d*-space) is a function of the stoichiometry of the pendant and is linearly dependent on the component mole fraction. Therefore, a certain *x* values can lead to consentaneous steric constraints such as *d* values between the two organic groups. The *x* value in CaPS-PVPA may play a

vital role in the confinement effect of the heterogeneous chiral Mn (III) salen catalysts, which will be discussed later for more detail.³¹

The models of $\text{Ca}(\text{NaPO}_4)_{1-x}[\text{PS-PVPA}]_x \cdot y\text{H}_2\text{O}$ series ($x = n(\text{organic phosphonic acid}) / [n(\text{inorganic phosphate}) + n(\text{organic phosphonic acid})]$), *viz.* where $x = 0.2, 0.25, 0.33, 0.4, 0.5, 0.75$ and 1 are deduced. The layers of the CaPS-PVPA is attributed to that each calcium atom is bonded to six oxygen atoms, and every three of these oxygen atoms are bonded to one phosphorus atom. The x value puts effect on the arrangement of P-G (B) group and P-OH (A) group, further on the steric configuration. For instance, a layer of CaPS-PVPA **5** ($x = 0.5$) reveal that there is a P-G (B) group inserted between two P-OH (A) or reverse on behalf of evacuating the higher-energy arrangement of pendant groups segregating on the interlayer. Based on this, the hypothesized model for CaPS-PVPA **5** may be simply denoted as “ABABAB...” And the scheme of the hypothesized cross section (Fig. 6) display that two bulky P-G (B) and four P-OH (A) groups are located around one P-G group. Meanwhile, bulky P-G groups are getting out of the layers owing to sterically directed energy. Similarly, the hypothesized model for CaPS-PVPA **3** ($x = 0.33$) can be denoted as “AABAABAAB...” And the scheme of the hypothesized cross section (Fig. 6) indicates that six small P-OH (A) groups are situated around one P-G group. Moreover, the d -space is larger than that of CaPS-PVPA **5** ($x = 0.5$), which can offer enough space for some larger substrates coordinating with the active sites. Obviously, steric hindrance between the substrates and active sites contribute to the confinement effect. Then the hypothesized model for CaPS-PVPA **2** ($x = 0.25$) can be denoted as “BAAABAAABAAA...”, and the scheme of the hypothesized cross section (Fig. 6) suggests that the space of two neighboring P-G groups is much larger than those of CaPS-PVPA **5** ($x = 0.5$) and CaPS-PVPA **3** ($x = 0.33$). Although there is large space for catalytic reaction, the confinement effect and the content of the active sites are decreased on the contrary.

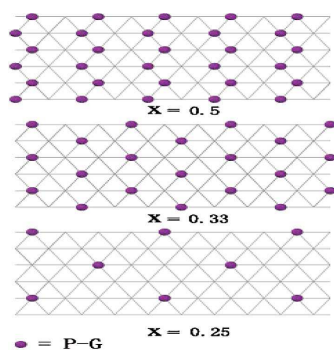


Fig. 6 The cross section of the $x = 0.25, x = 0.33$ and $x = 0.5$.

Qualitatively, changes in the d spacing with composition can be legitimate in terms of correlative factors that are subordinate to the steric interactions of the bulkier styrene-phenylvinylphosphonic acid copolymer groups and the conformations of the organic groups. According to CaPS-PVPA, the styrene-phenylvinylphosphonic acid copolymer chains are located on the

external surfaces or between the layers of CaPS-PVPA. If the x values are large, such as CaPS-PVPA **6** ($x = 0.75$) or more, the space between two styrene-phenylvinylphosphonic acid copolymer groups will be small. To refrain from the higher-energy arrangement of pendant groups segregating on the interlayer, most of the styrene-phenylvinylphosphonic acid copolymer groups are pushed out and located on the external surface of CaPS-PVPA. In contrast, if x values are relatively small, for instance CaPS-PVPA **3** ($x = 0.33$) and CaPS-PVPA **2** ($x = 0.25$) or less, the space between two styrene-phenylvinylphosphonic acid copolymer groups will be large, which agree with the results originated in XRD. And then, more parts of the styrene-phenylvinylphosphonic acid copolymer groups are naturally located between the layers of CaPS-PVPA. In a word, the frameworks of CaPS-PVPA may be easily designed and assembled to generate pores or channels with various sizes and shapes by appropriate modification of the styrene-phenylvinylphosphonic acid copolymer chain. In addition, the porous hosted materials put effect on catalytic disposition owing to a synergistic effect of the nanoporous solid, the linker, and chiral

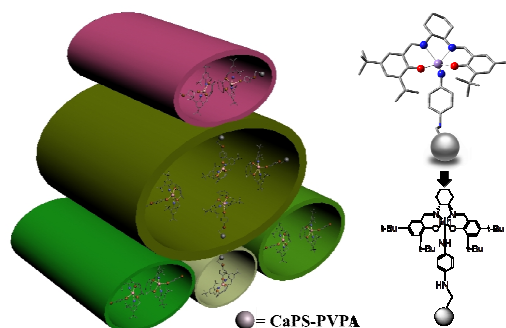


Fig. 7 The hypothesized structure of the heterogeneous catalyst

salen Mn (III) (Fig.7).²⁵ Mesoporous materials are reckoned as most applicable supports for the immobilization of Mn-salen complexes.³² Maybe the special structures of CaPS-PVPA contribute to the superior catalytic ability.

Catalytic properties

Catalytic results reveal comparable or even higher enantioselectivities than those of corresponding homogeneous catalysts or some other supported catalysts reported before such as the immobilized chiral salen Mn (III) onto ZPS-IPPA modified by aryldiamine (Table 4). The performance of catalyst A is significant higher than that of catalyst B and C prepared by our group before. Further researches were under way.

The homogeneous catalyst C indicates higher ee value than that of the Jacobsen's catalyst (ee, 90.8-54%), which manifests that the rigid linker is devoted to the increase of ee values. Moreover, the ee values further increases from 90.8% to >99% after the homogeneous catalyst E immobilized onto CaPS-PVPA (A). In a word, the whole immobilized chiral salen Mn(III) catalysts include the support CaPS-PVPA, the rigid linkers and chiral salen Mn altogether contributed to the increase of ee values.

Table 4 Asymmetric epoxidation of α -methylstyrene and indene catalyzed by heterogeneous catalysts with *m*-CPBA/NMO^a as oxidative system

Entry	Substrate	Catalyst	Time	Con. (%)	Ee (%)
1	α -methylstyrene	A	6	>99	>99
2	α -methylstyrene	B	6	56	18
3	α -methylstyrene	C	6	64	90.8
4	indene	A	6	>99	>99
5	indene	B	6	62	59
6	indene	C	6	98.7	83.7

^a Reactions were carried out at -20°C in CH₂Cl₂ (4 mL) with α -methylstyrene (1 mmol) or indene (1 mmol), *n*-nonane (internal standard, 1 mmol), NMO (5 mmol), homogeneous (5 mol%) or heterogeneous salen Mn(III) catalysts (5 mol%) and *m*-CPBA (2 mmol). The conversion and the ee value were determined by GC with chiral capillary columns HP19091GB213, 30 m × 0.32 mm × 0.25 μ m.

A = the immobilized chiral salen Mn(III) catalysts on *p*-Phenylenediamine modified CaPS-PVPA.

B = the immobilized chiral salen Mn(III) catalysts on *p*-Phenylenediamine modified ZPS-IPPA

C = the homogeneous chiral salen Mn(III) catalyst modified by *p*-phenylenediamine³³

Shown in Table 5, the yield and the enantioselectivity decrease slightly after recycling for nine times and still give conversion (90%) and enantioselectivity (87%) (Table 5). The effective separation of the chiral Mn(III) salen complexes by the solid support CaPS-PVPA contribute to the superior stability of the heterogeneous chiral Mn(III) salen catalyst in the case that they would dimerize to form the inactive *m*-oxo-Mn(IV) species. The decrease of the yield could be ascribed to the decomposition of the chiral Mn(III) salen complex under epoxidation conditions, and the loss of the hyperfine granules of the heterogeneous chiral Mn(III) salen catalysts.

Table 5 The recycles of catalyst^a in the asymmetric epoxidation of α -methylstyrene^b

Run	Time (h)	Con. (%)	ee (%) ^c
1	5	>99	>99
2	5	>99	>99
3	5	>99	>99
4	5	>99	>99
5	5	98	>99
6	5	97.5	>99
7	5	95	97
8	5	93	95
9	5	90	87
10	5	88	80
11	5	83	72
12	5	76	36

^a The catalyst is the immobilized chiral salen Mn(III) catalysts on *p*-Phenylenediamine modified CaPS-PVPA

^b Reactions were carried out at -40 °C in CH₂Cl₂ (2 mL) with α -methylstyrene (1 mmol), *n*-nonane (internal standard, 1 mmol), *m*-CPBA (0.38 mmol), heterogeneous salen Mn(III) catalysts (5 mol%). The conversion and the ee value were determined by GC with chiral capillary columns HP19091GB213, 30 m × 0.32 mm × 0.25 μ m.

^c Same as in Table 4.

As can be seen in Table 6, the conversion and enantioselectivity maintain at the same level for the large-scale reactions under whichever condition that the large scale is 50 times or 100 times as much as the experimental scale.

Table 6 Large-scale asymmetric epoxidation of α -methylstyrene^a

Entry	Time (h)	Con. (%)	ee ^d (%)
1 ^b	5	>99	>99
2 ^c	5	>99	>99

^a Reactions were carried out at -40°C in CH₂Cl₂ with α -methylstyrene, *n*-nonane, *m*-CPBA, heterogeneous salen Mn(III) catalysts (5 mol%). The conversion and the ee value were determined by GC with chiral capillary columns HP19091G-B213, 30 m × 0.32 mm × 0.25 μ m.

^b The usage amounts of reagents were α -methylstyrene (50 mmol), *n*-nonane (50 mmol), heterogeneous catalyst (0.5 mmol), *m*-CPBA (100 mmol), respectively.

^c The usage amounts of reagents were α -methylstyrene (100 mmol), *n*-nonane (100 mmol), heterogeneous catalyst (5 mmol), *m*-CPBA (200 mmol), respectively.

^d Same as in Table 4.

Conclusions

In summary, a facile, cost-effective and environmentally friendly route was developed to prepare hybrid material CaPS-PVPA by employing well-established synthetic procedures. The correlation between the ratio of organic phosphonate to inorganic phosphate and the density/structural dimensionality of the products were systemically studied. And the hypothesized structure of CaPS-PVPA and a confinement effect of nanopores are proposed. To investigate the structure-property relationship, the as-prepared hybrid material was further employed as catalyst support in asymmetric epoxidation of non-functionalized olefins. The superior catalytic performance endues CaPS-PVPA with promising heterogeneous catalyst supports in the immobilization of chiral salen Mn(III).

Acknowledgements

This work is financially supported by the Fundamental Research Funds for the Central Universities (XDJK2013C120) and the Xihua University Key Projects (Z1223321) and Sichuan Province Applied Basic Research Projects (2013JY0090) and the Department of Education of Sichuan Province Projects (13ZB0030) and Chongqing Special Funding for Postdoctoral (Xm2014028) and Chongqing Postdoctoral Daily Fund (Rc201419).

References

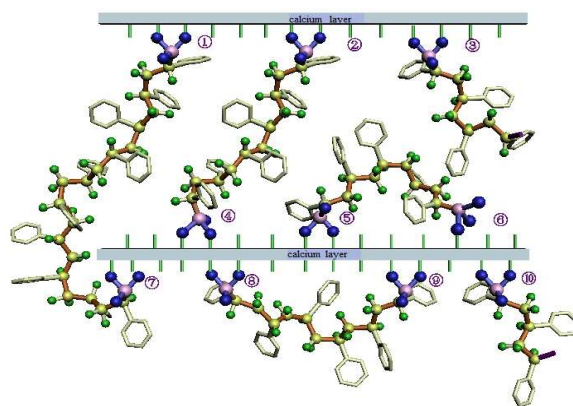
- B. Chen, N.W. Ockwig, A. R. Millward, D.S. Contreras, O.M. Yaghi, *Angew. Chem., Int. Ed. Engl.*, 2005, **44**, 4745.
- J. L. C. Rowsell, O.M. Yaghi, *Angew. Chem., Int. Ed. Engl.*, 2005, **44**, 4670.
- D. Bradshaw, J. B. Claridge, E. J. Cussen, T. J. Prior, M. J. Rosseinsky, *Chem. Res.*, 2005, **38**, 273.
- O. Ohmori, M. Kawano, M. Fujita, *Angew. Chem., Int. Ed.*, 2005, **44**, 1962.
- E. Y. Lee, S. Y. J ang, M. P. Suh, *J. Am. Chem. Soc.*, 2005, **127**, 6374.
- Z. Wang, B. Zhang, M. Kurmoo, M. A. Green, H. Fujiwara, T. Otsuka, H. Kobayashi, *Inorg. Chem.*, 2005, **44**, 1230.
- H. Kim, M.P. Suh, *Inorg. Chem.*, 2005, **44**, 810.

- 8 R. Kitaura, S. Kitagawa, Y. Kubota, T.C. Kobayashi, K. Kindo, Y. Mita, A. Matsuo, M. Kobayashi, H.-C. Chang, T.C. Ozawa, M. Suzuki, M. Sakata, M. Takata, *Science*, 2002, **298**, 2358.
- 9 D. Bradshaw, T. J. Prior, E. J. Cussen, J. B. Claridge, M. J. Rosseinsky, *J. Am. Chem. Soc.* 2004, **126**, 6106.
- 10 A. Cingolani, S. Galli, N. Masciocchi, L. Pandolfo, C. Pettinari, A. Sironi, *J. Am. Chem. Soc.*, 2005, **127**, 6144.
- 11 E.Y. Lee, S.Y. Jang, M.P. Suh, *J. Am. Chem. Soc.*, 2005, **127**, 6374.
- 12 C. Janiak, *Dalton Trans.*, 2003, 2781 (and references therein).
- 13 D. B. Mitzi, *Dalton Trans.* 2001, 1.
- 14 R. Q. Zeng, X. K. Fu, C. B. Gong, Y. Sui, X. B. Ma, X. B. Yang, *J. mol. Catal. A*, 2005, **229**, 1.
- 15 X. B. Ma, X. K. Fu, *J. mol. Catal. A*, 2004, **208**, 129.
- 16 W. S. Ren, X. K. Fu, H. B. Bao, R. F. Bai, P. P. Ding and B. L. Sui, *Catal. Commun.*, 2009, **10**, 788.
- 17 X. B. Tu, X. K. Fu, Hu, X. Y. Hu, Y. D. Li, *Inorganic Chemistry Communications*, 2010, **13**, 404.
- 18 B. W. Gong, X. K. Fu, J. X. Chen, Y. D. Li, X. C. Zou, X. B. Tu, P. P. Ding and L. P. Ma, *J. Catal.*, 2009, **262**, 9.
- 19 J. Huang, X. K. Fu, G. Wang, C. Li, X. Y. Hu, *Dalton. Trans.*, 2011, **40**, 3631.
- 20 J. Huang, X. K. Fu, G. Wang, Q. Miao, *Dalton Trans.*, 2012, **41**, 10661.
- 21 Brown P. W. Calcium Phosphates in Biomedical Engineering. In: *Encyclopedia of Materials: Science and Technology (Second Edition)*. Oxford: Elsevier 2001. 893-7.
- 22 K. M. Parida, K.G. Mishra, S.K. Dash, *Ind. Eng. Chem. Res.* 2012, **51**, 2235.
- 23 W. Zhang, N. H. Lee, E. N. Jacobsen, *J. Am. Chem. Soc.*, 1994, **116**, 425.
- 24 B. W. Gong, X. K. Fu, H. S. Shen, L. H. Ma, Y. J. Xia, *Fine. Chem.*, 2008, **25**, 603.
- 25 J. Huang, X. K. Fu, Q. Miao, *Appl. Catal: A*, 2011, 407, 163. 25
- 26 H. D. Zhang, C. Li, *Tetrahedron*, 2006, **62**, 6640.
- 27 F. Rajabi, S. Naserian, A. Primo, R. Luque, *Adv. Synth. Catal.*, 2011, **353**, 2060.
- 28 V. J. MAYANI, S. H. R. ABDI, S. V. MAYANI, H. C. KIM, S. K. PARK, *Chirality*, 2011, **23**, 300.
- 29 Y. Liu, V. Piñón III, M. Weck, *Polym. Chem.*, 2011, **2**, 1964.
- 30 C. Li, H. D. Zhang, D. M. Jiang, Q. H. Yang, *Chem. Commun.*, 2007, **6**, 547.
- 31 W. S. Ren, X. K. Fu, *J. Mol. Catal. A: Chem.*, 2009, **312**, 40.
- 32 H. D. Zhang, S. Xiang, C. Li, *Chem. Commun.*, 2005, **9**, 1209.
- 33 J. Huang, X. K. Fu, Q. Miao, *Catal. Sci. Technol.*, 2011, **1**, 1472.

Graphic Abstract

A novel, facile method to prepare hybrid calcium poly(styrene-phenylvinyl-phosphonate)-phosphate material for superior performance catalyst support

Jing Huang, Mei Tang, Jian Ming Yao, Xin Li and Chang Ming Li*



Various pores or channels produced by modification of PS-PVPA chain could contribute to significant impact on the excellent catalytic activity.